This is a repository copy of *Analysis and Recognition of Three Dimensional Closed Boundaries.*.

White Rose Research Online URL for this paper:
http://eprints.whiterose.ac.uk/79635/

Monograph:

Tsang, K.M., To, F.W. and Billings, S.A. (1994) Analysis and Recognition of Three Dimensional Closed Boundaries. Research Report. ACSE Research Report 519 . Department of Automatic Control and Systems Engineering

Analysis and recognition of three dimensional closed boundaries

K. M. Tsang[*]

F. W. To[*]

and

S. A. Billings[†]

[*]Department of Electrical Engineering
Hong Kong Polytechnic
Hung Hom
Kowloon
Hong Kong

[†]Department of Automatic Control and Systems Engineering
University of Sheffield
Sheffield S1 3JD
UK

Abstract

An autoregressive model is introduced for modelling, invariant feature extraction and recognition of arbitrary three dimensional (3D) closed boundary curves. An orthogonal estimation algorithm is derived for the estimation of the coefficient matrix associated with the model and an error reduction ratio is used to detect the order of the model. It is shown that the eigenvalues and the determinant of the coefficient matrix are invariant to rotation around the origin, to the choice of starting point in tracing the boundary, and to scale and translation which can therefore be extracted for the recognition of the 3D closed boundary curves.

1. Introduction

In the areas of robotics and machine vision there is a growing interest in developing efficient procedures for the modelling and recognition of 3D objects (Sadjadi and Hall 1980, Oshima and Shirai 1983, and Bhanu 1984). The choice of a proper representation scheme is critical to the manipulation of the image data in these applications. The enclosing surface of a well behaved 3D rigid solid unambiguously specifies the object and surface characteristics are therefore useful in shape dominated pattern recognition. However in practice, many 3D objects can be represented and recognised based on the boundary curves alone and a full surface description of the object may not be necessary for the recognition of the object.

There are numerous techniques available for the analysis and recognition of 2D shapes. Shape descriptions have been used with notable success with a variety of descriptors appearing in the literature such as the Fourier descriptors (Zahn and Roskies 1972), moment invariants (Dundani el al 1977) and the autoregressive (AR) model approach (Dubois and Glanz 1986, Sekita et al 1992, and Tsang and Billings 1994). However the application of 2D techniques to 3D curves may give erroneous results for modelling and classification of 3D objects. Hence it is desirable to have an efficient way of representing and recognising 3D boundary curves. In the present study, the AR model approach is extended to cover the modelling of 3D closed boundaries. The orthogonal estimation algorithm developed for the analysis of 2D shape (Tsang and Billings 1994) is extended to cover 3D boundary curves and procedures that determine the order and the significant lagged terms in the AR model are introduced using an error reduction ratio test. If the order of the model is insufficient to capture the characteristics of the boundary data points, more lagged terms can be added to the model with the advantage that the newly introduced parameters will not affect the previously estimated orthogonal parameters. Using the orthogonal estimator and the error reduction ratios a minimum set of feature vectors can therefore be derived and this should considerably reduce the computational time for the classification of 3D boundary shapes. A new recognition algorithm based on the estimated AR coefficient matrix is derived such that the recognition is invariant to rotation, size and translation of an object. Simulated examples are included to demonstrate the performance of the algorithms.

2. Autoregressive model representation of a 3D boundary

There are currently numerous techniques for acquiring information about surface and boundary geometry from a variety of sensors (Jarvis 1983). These typically provide information only about the visible surface of an object. For complete 3D surface and

boundary data information from multiple partial views is required. This is done by using an active observer (Aloimonus et al 1987) or a mechanism for rotating the object in front of a passive observer. Assuming that full 3D surface or boundary data is available, an AR model representation of the closed boundary curve can be obtained. Let $U(k) = [X(k)\ Y(k)\ Z(k)]^T$, $k=0,1,...,N-1$ be a sequence of 3D boundary data points obtained by sampling according to the order of tracing by a sequential boundary follower. The distance between any consecutive data points is fixed and $X(k) = X(k+N)$, $Y(k) = Y(k+N)$ and $Z(k) = Z(k+N)$. An AR model can then be fitted to the N collected data records. However the fitted AR model based on the raw data records will be dependent upon transformations of the boundary such as translation, scale and rotation. For invariance, the sampled means are first subtracted from the raw data records to give

$$\begin{aligned} x(k) &= X(k) - \overline{X(k)} \\ y(k) &= Y(k) - \overline{Y(k)} \\ z(k) &= Z(k) - \overline{Z(k)} \end{aligned} \tag{1}$$

where the overbar denotes data averaging and a state vector $u(k) = [x(k)\ y(k)\ z(k)]^T$ is constructed. Hence $u(k)$ will be a sequence of equally spaced 3D boundary data points as shown in Fig. 1. An AR model of order m is formed from this sequence of boundary points by combining the preceding m boundary points to give

$$u(k) = \sum_{i=1}^{m} A_i u(k-i) + \epsilon(k) \tag{2}$$

where $\epsilon(k)$ is an error sequence and A_i, $i=1,...,m$ are m 3×3 coefficient matrices associated with the AR model. Notice that eqn.(2) will be invariant to translation because any translation will be removed after the operation of eqn.(1).

3. Properties of the AR model

The coefficient matrix A_i will have some invariant properties. When each boundary point is represented by a state vector $u(k)$, any similarity transformations such as rotation about the origin, scale up or down etc. can be expressed as pre-multiplying each boundary point by the similarity transformation matrix B to give

$$Bu(k) = \sum_{i=1}^{m} BA_i u(k) + B\epsilon(k) \tag{3}$$

Since B is nonsingular and its inverse exists (Kreyszig 1979), eqn.(3) can be written as

2

$$u'(k) = \sum_{i=1}^{m} BA_i B^{-1} u'(k-i) + \epsilon'(k) \qquad (4)$$

where $u'(k) = Bu(k)$ and $\epsilon'(k) = B\epsilon(k)$. Comparing eqn.(4) with eqn.(2), the coefficient matrix changes from A_i to $BA_i B^{-1}$. Consider the eigenvalues of the matrix $BA_i B^{-1}$

$$\det(\lambda I - BA_i B^{-1}) = \det(B(\lambda I - A_i)B^{-1})$$
$$= \det(B)\det(B^{-1})\det(\lambda I - A_i) = \det(\lambda I - A_i)$$

where λ denotes eigenvalue and det(.) the determinant. Since B is a similarity transformation matrix the eigenvalues, determinant and trace of A_i will be the same as $BA_i B^{-1}$ (Kreyszig 1979). The eigenvalues, trace values and determinants of the AR coefficient matrix can therefore be extracted for the recognition of 3D boundary curves providing an efficient way of estimating the AR coefficient matrix is available.

4. The orthogonal estimator

The orthogonal least squares estimator (Tsang and Billings 1994) has been successfully adapted for the analysis and recognition of 2D boundary curves. The algorithm is efficient and robust. The error reduction ratio, which is incorporated as part of the orthogonal estimator, provides an effective way of assessing the significance of model terms. This provides a very flexible procedure for ordering the terms corresponding to the contribution that each makes to the 3D pattern. Prior to the application of the orthogonal estimation algorithm to the estimation of the AR coefficient matrix, eqn.(2) is first split into three scalar model to give

$$x(k) = \sum_{i=1}^{m} [(a_{11})_i x(k-i) + (a_{12})_i y(k-i) + (a_{13})_i z(k-i)] + \epsilon_x(k) = \sum_{i=1}^{3m} \theta_{xi} p_{xi}(k) + \epsilon_x(k)$$

$$y(k) = \sum_{i=1}^{m} [(a_{21})_i x(k-i) + (a_{22})_i y(k-i) + (a_{23})_i z(k-i)] + \epsilon_y(k) = \sum_{i=1}^{3m} \theta_{yi} p_{yi}(k) + \epsilon_y(k) \qquad (5)$$

$$z(k) = \sum_{i=1}^{m} [(a_{31})_i x(k-i) + (a_{32})_i y(k-i) + (a_{33})_i z(k-i)] + \epsilon_z(k) = \sum_{i=1}^{3m} \theta_{zi} p_{zi}(k) + \epsilon_z(k)$$

where $(a_{jk})_i$ is the jk element of the matrix A_i, $\epsilon_x(k)$, $\epsilon_y(k)$ and $\epsilon_z(k)$ are the estimation errors for the sequences $x(k)$, $y(k)$ and $z(k)$, θ_{xi}, θ_{yi} and θ_{zi} are the coefficients associated with the regression terms $p_{xi}(k)$, $p_{yi}(k)$ and $p_{zi}(k)$ respectively in the expansion of eqn.(2) and $p_{xi}(k), p_{yi}(k)$ and $p_{zi}(k)$ represent any one of the lagged terms $x(k-i), y(k-i)$ and $z(k-i)$. For

example, a first order AR model can be written as

$$x(k) = (a_{11})_1 x(k-1) + (a_{12})_1 y(k-1) + (a_{13})_1 z(k-1) + \epsilon_x(k)$$

$$y(k) = (a_{21})_1 x(k-1) + (a_{22})_1 y(k-1) + (a_{23})_1 z(k-1) + \epsilon_y(k)$$

$$z(k) = (a_{31})_1 x(k-1) + (a_{32})_1 y(k-1) + (a_{33})_1 z(k-1) + \epsilon_z(k)$$

where

$$\theta_{x1} = (a_{11})_1 \quad , \quad \theta_{x2} = (a_{12})_1 \quad , \quad \theta_{x3} = (a_{13})_1$$
$$\theta_{y1} = (a_{21})_1 \quad , \quad \theta_{y2} = (a_{22})_1 \quad , \quad \theta_{y3} = (a_{23})_1$$
$$\theta_{z1} = (a_{31})_1 \quad , \quad \theta_{z2} = (a_{32})_1 \quad , \quad \theta_{z3} = (a_{33})_1$$
$$p_{x1}(k) = p_{y1}(k) = p_{z1}(k) = x(k-1)$$
$$p_{x2}(k) = p_{y2}(k) = p_{z2}(k) = y(k-1)$$
$$p_{x3}(k) = p_{y3}(k) = p_{z3}(k) = z(k-1)$$

The orthogonal estimation algorithm involves transforming eqn.(5) into three auxiliary equations

$$x(k) = \sum_{i=1}^{3m} g_{xi} w_{xi}(k) + \epsilon_x(k)$$

$$y(k) = \sum_{i=1}^{3m} g_{yi} w_{yi}(k) + \epsilon_y(k) \tag{6}$$

$$z(k) = \sum_{i=1}^{3m} g_{zi} w_{zi}(k) + \epsilon_z(k)$$

where g_{xi}, g_{yi} and g_{zi} are constant coefficients associated with the orthogonal data sets $w_{xi}(k)$, $w_{yi}(k)$ and $w_{zi}(k)$ respectively and the orthogonality conditions

$$\overline{w_{xi}(k)w_{xj}(k)} = \overline{w_{yi}(k)w_{yj}(k)} = \overline{w_{zi}(k)w_{zj}(k)} = 0 \quad , \quad i \neq j \tag{7}$$

hold where the overbar denotes data averaging. Consider first the model related to the sequence $x(k)$, a set of orthogonal data records can be constructed using the formulae (Korenberg et al 1988, Tsang and Billings 1994)

$$w_{x1}(k) = p_{x1}(k)$$

$$w_{xi}(k) = p_{xi}(k) - \sum_{j=1}^{i-1} \alpha_{xji} w_{xj}(k) \quad , \quad j < i$$

$$\alpha_{xji} = \overline{w_{xj}(k)p_{xi}(k)} \Big/ \overline{w_{xj}^2(k)} \quad , \quad j=1,...,i-1 \tag{8}$$

$$g_{xi} = \overline{x(k)w_{xi}(k)} \Big/ \overline{w_{xi}^2(k)} \quad , \quad i=1,...,3m$$

Note that the orthogonal coefficients g_{xj} only depend upon the previously fitted orthogonal parameters and will not be affected by any new term. The orthogonal parameters will therefore be invariant to the specified model order. Once g_{xj} have been estimated, the elements of the AR coefficient matrix related to the sequence $x(k)$ can be recovered as (Korenberg et al 1988, Tsang and Billings 1994)

$$\theta_{x3m} = g_{x3m}$$

$$\theta_{xj} = g_{xj} - \sum_{i=j+1}^{3m} \alpha_{xji} \theta_{xi} \; , \; j=3m-1,...,1 \tag{9}$$

Equations (8) and (9) define the orthogonal least squares algorithm for the analysis of the sequence $x(k)$. They could equally be applied to the sequences $y(k)$ and $z(k)$ to obtain the corresponding coefficients of the AR matrix relating to these sequences such that the full AR model describing the 3D boundary curve can be reconstructed from the estimated parameters and the characteristics of the parameter matrix such as eigenvalues, trace and determinants can be readily extracted for the analysis and recognition of 3D boundary curves.

The error reduction ratio which is a by-product of the orthogonal least squares estimator can provide information regarding both the significance of individual variables in the system model and the adequacy of the fitted model. The percentage reduction in the output variance as a result of including the term $g_{xj} w_{xj}(k)$ into the model for the sequence $x(k)$ can be expressed in terms of the error reduction ratio

$$\epsilon RR_{xj} = 100 \, g_{xj}^2 \, \overline{w_{xj}^2(k)} \, / \, \overline{x^2(k)} \tag{10}$$

If the value of ϵRR_{xj} is large, this would imply that the term $g_{xj} w_{xj}(k)$ is a good candidate to characterise the boundary model and if ϵRR_{xj} is less than a certain threshold, say 0.01, the term can be excluded from the estimation. Also if the sum of ϵRR_{xj} values for the selected terms is close to 100, this would be an indication that the orthogonal model adequately represents the sampled boundary data points.

From eqn.(8), the estimated coefficients α_{xji} and g_{xj} are governed by averaging values. If the equally sampled boundary data records are sufficiently fine, the average values should approach the actual mean value of the boundary data points and the estimated coefficients will be independent of the starting point in tracing the boundary curve.

5. Methods of recognising shapes

The eigenvalues, trace values and determinants of the AR coefficient matrix are invariant to translation of a boundary if the origin is set at the boundary centroid. To make the eigenvalues, trace values and determinants invariant to the scale of a boundary the number of boundary points is fixed to N and the boundary is divided into N segments of equal arc length. It is expected that the eigenvalues for the same shape will be identical because they are theoretically invariant under the similarity transformation. Thus shapes could be classified by using the Euclidean distance between the tested eigenvalues, trace values and determinants of the AR model and the reference values. Using the Euclidean distance between the tested parameter vectors λ'_i, $trace(A'_i)$ and $det(A'_i)$ against the reference vector $\{\lambda^c_i, trace(A^c_i), det(A^c_i), c=1,...,C\}$ where C is the number of different classes of boundary curves should therefore provide a simple means of classification. The tested boundary points $u'(k)$ are classified as belonging to the class Q if the Euclidean distance between the feature vectors is a minimum

$$\sum_{i=1}^{m} \sqrt{|\lambda'_{i1}-\lambda^Q_{i1}|^2 + |\lambda'_{i2}-\lambda^Q_{i2}|^2 + |\lambda'_{i3}-\lambda^Q_{i3}|^2}$$

$$= \min\left\{\sum_{i=1}^{m} \sqrt{|\lambda'_{i1}-\lambda^c_{i1}|^2 + |\lambda'_{i2}-\lambda^c_{i2}|^2 + |\lambda'_{i3}-\lambda^c_{i3}|^2}, c=1,...,C\right\} \rightarrow u'(k)\in Q$$

$$\sum_{i=1}^{m} |trace(A'_i)-trace(A^Q_i)|$$

$$= \min\left\{\sum_{i=1}^{m} |trace(A'_i)-trace(A^c_i)|, c=1,...,C\right\} \rightarrow u'(k)\in Q$$

$$\sum_{i=1}^{m} |det(A'_i)-det(A^Q_i)|$$

$$= \min\left\{\sum_{i=1}^{m} |det(A'_i)-det(A^c_i)|, c=1,...,C\right\} \rightarrow u'(k)\in Q$$

(11)

Once the shape has been recognised, the orientation of the object can also be identified. The starting point of the data sequence is arbitrary but in order to identify the angle of rotation of an object the alignment of the tested sequence with the reference sequence is required. A cyclic correlation is therefore performed on the radius vector of the tested sequence and the reference radius vector $r(k) = \sqrt{x^2(k)+y^2(k)+z^2(k)}$ to give

6

$$\psi_{r'r}(\tau) = \cfrac{\dfrac{1}{N}\sum_{k=0}^{N-1}\left(r'(k)-\overline{r'(k)}\right)\left(r(k+\tau)-\overline{r(k+\tau)}\right)}{\sqrt{\dfrac{1}{N}\sum_{k=0}^{N-1}\left(r'(k)-\overline{r'(k)}\right)^2}\sqrt{\dfrac{1}{N}\sum_{k=0}^{N-1}\left(r(k)-\overline{r(k)}\right)^2}} \quad,\ r'(k)=r'(N+k)\ ,\ r(k)=r(N+k) \quad (12)$$

$\psi_{r'r}(\tau)$ will give a maximum value if the two sequences are aligned. Once the alignment factor τ_{max} is found, the orientation of the tested boundary can be evaluated as

$$u'(k) = Bu(k+\tau_{max}) \tag{13}$$

A least squares estimate for B can be obtained as

$$B^T = (\underline{u}'\underline{u}'^T)^{-1}(\underline{u}'\underline{u}'^T) \quad,\quad \underline{u}'^T = \begin{bmatrix} u'(1)^T \\ u'(2)^T \\ \vdots \end{bmatrix} \quad,\quad \underline{u}^T = \begin{bmatrix} u(\tau_{max}+1)^T \\ u(\tau_{max}+2)^T \\ \vdots \end{bmatrix} \tag{14}$$

Hence orientation and size can be extracted from B.

6. Boundary on a plane

The equation of a plane is given by

$$px(k) + qy(k) + rz(k) = s \tag{15}$$

where p, q, r, and s are constant coefficients. From eqn.(15), any one of the variables $x(k)$, $y(k)$ and $z(k)$ can be derived from the knowledge of the other two variables if p, q, r and s are fixed. The inclusion of the term $z(k)$ in the modelling of a 3D boundary curve situated on a plane will therefore be redundant because $z(k)$ can be absorbed by the other two variables $x(k)$ and $y(k)$. In the orthogonalisation procedure, after the first two orthogonalisation steps using the variables $x(k)$ and $y(k)$, the inclusion of the term $z(k)$ will provide no further information on the shape of an object if the curve is situated on a plane because the contribution has already been absorbed by the variables $x(k)$ and $y(k)$. The zero or close to zero contribution of any consistent terms in the orthogonalisation procedure should therefore be a good indicator for detecting if the boundary curve falls on a plane. Notice that the inclusion of these redundant terms into the model will tend to introduce numerical problems in the reconstruction of the coefficient matrix. To avoid this problem, a procedure has to be introduced such that if the contribution of a particular term is zero, or less than a very small threshold, that term will be excluded from the estimation and the formulation of the AR coefficient matrix and the corresponding coefficient will be set to zero so that the eigenvalues, trace and determinant can be extracted for the recognition

7

of the boundary. Better still the recognition can be reduced to a two dimensional recognition problem by throwing away the third redundant term in the estimation such that the AR coefficient matrix is reduced to a 2X2 matrix and an equation of a plane is fitted to the collected data. Consider for example the two plane shapes with different orientations shown in Fig.2 where 100 boundary data records were sampled from the two shapes for further analysis. From the error reduction ratio tests, a second order AR model was sufficient to describe the curve because the sum of the error reduction ratio tests was over 99.9%. Further, the error reduction ratio tests revealed that two variables were sufficient to capture the feature of the shape and the third dimension variable was redundant because the contribution to the error reduction ratio was close to zero. Hence a second order AR model with a 2X2 coefficient matrix was fitted to the collected data set of Fig.2a) and the estimated AR model was given by

$$\begin{bmatrix} x(k) \\ y(k) \end{bmatrix} = \begin{bmatrix} 1.8735 & 0.0212 \\ 0.0084 & 1.9443 \end{bmatrix} \begin{bmatrix} x(k-1) \\ y(k-1) \end{bmatrix} + \begin{bmatrix} -0.8778 & -0.0156 \\ -0.1210 & -0.9598 \end{bmatrix} \begin{bmatrix} x(k-2) \\ y(k-2) \end{bmatrix} + \begin{bmatrix} \epsilon_x(k) \\ \epsilon_y(k) \end{bmatrix} \quad (16)$$

The eigenvalues, trace values and determinant for the two matrices are given by $\lambda_{A_1} = (1.8711, 1.9467)$, $trace(A_1) = 3.8178$, $det(A_1) = 3.6425$, $\lambda_{A_2} = (-0.8756, -0.9621)$, $trace(A_2) = -1.8376$, $det(A_2) = 0.8423$ and the shape was situated on the plane $z(k) = 0$. Fig.2b) was obtained from Fig.2a) using the similarity transformation matrix

$$B = \begin{bmatrix} 0.2198 & 0.2620 & 0.9397 \\ -.9264 & 0.3578 & 0.1170 \\ -.3056 & -.8963 & 0.3214 \end{bmatrix}$$

For 100 collected data records from the curve in Fig.2b) the orthogonal estimation algorithm produced the second order AR model

$$\begin{bmatrix} x(k) \\ y(k) \end{bmatrix} = \begin{bmatrix} 1.9429 & 0.0141 \\ 0.0198 & 1.8750 \end{bmatrix} \begin{bmatrix} x(k-1) \\ y(k-1) \end{bmatrix} + \begin{bmatrix} -.9531 & -.0145 \\ -.0479 & -.8845 \end{bmatrix} \begin{bmatrix} x(k-2) \\ y(k-2) \end{bmatrix} + \begin{bmatrix} \epsilon_x(k) \\ \epsilon_y(k) \end{bmatrix} \quad (17)$$

and the equation of the plane fitted to Fig.2b) with the mean removed was given by

$$z(k) = -2.9238x(k) - 0.3640y(k) \quad (18)$$

The eigenvalues, traces and determinants of the coefficient matrix for eqns.(16) and (17) are exactly the same. This clearly demonstrates that if the boundary curve falls on a plane the recognition procedure reduces to the operation of a 2X2 coefficient matrix and the zero contribution of the third dimension variable indicates that the shape lies on a plane.

7. Experiments and results

The effectiveness of the estimation algorithm in the recognition of 3D boundary curves will be investigated using several examples. The experiments are principally concerned with simply connected shapes which are completely known. The shapes used for the experiments are illustrated in Figs. 3 and 4. Samples with various sizes and different translational and rotational position were collected. The sizes were varied from 0.4 to 1.1. Shape set A of Fig.3 is composed of 9 boundary curves of different sizes and orientations which were used to investigate if the eigenvalues, trace values and determinants of the AR model fitted to the 3D boundary data are invariant to similarity transformation and can be used for pattern recognition. Shape set B (Fig.4) is composed of 9 shapes where some are relatively similar. This serves to test the sensitivity of the shape model to small variations in object shape.

7.1 Classification results and discussion

To investigate the effects of translation, size and rotation on the AR model, nine views obtained from the same pattern with different orientations and sizes were used (Fig.2). 100 boundary sampled data were obtained from the nine curves and the orthogonal estimation algorithm was applied. From the error reduction ratio test, a second order AR model was sufficient to described the curve because from the error reduction ratio test, a second order AR model captured over 99.9% of the total output variance. Figure 5 shows the eigenvalues, trace values and determinants of the fitted AR coefficient matrix for the nine curves. They are very similar and this clearly demonstrates that the recognition algorithm is invariant to size, translation and rotation.

In order to estimate the relative size and orientation of a particular object, view (5) was selected for the analysis and view (1) of shape set A was taken as the reference. One hundred sampled data were used for the analysis. The relative size of view (5) to view (1) can be obtained by

$$\sum_{k=1}^{100} r'(k) \bigg/ \sum_{k=1}^{100} r(k) = 0.8$$

To evaluate the orientation of the object, a cyclic correlation was performed on the radius vectors for views (5) and (1) and the correlation function is shown in Fig.6. The correlation function is a maximum when $\tau = 41$ and, from eqn.(4), the similarity transformation matrix was given by

$$B = \begin{bmatrix} -.2989 & 0.5294 & 0.5150 \\ -.4851 & -.5574 & 0.3170 \\ 0.5810 & 0.3170 & 0.5104 \end{bmatrix}$$

Figure 7 illustrates the sampled boundary data points of view (5) superimposed on the transformed reference view. A very close match between the two curves has clearly been obtained.

Shape set B of Fig.4 contains nine different objects. Some of the shapes are very similar and some are rather complicated. This serves to test the performance of the algorithm when used to classify a large number of patterns. One hundred boundary points were collected for each pattern shown in Fig.4 and the estimated eigenvalues, trace values and determinants of the fitted AR coefficient matrix are shown in Fig.8. The Euclidean distances between the nine patterns are shown in Fig.9 and they indicate a similarity between curves 5,6 and 7 because the Euclidean distances between these parameter vectors are small. Finally 81 patterns of different sizes, and orientations created from Fig.4 were used to test the classification rule and the algorithm correctly classified them all.

8. Conclusions

The orthogonal estimation algorithm provides an effective approach for estimating the coefficient matrix associated with the AR model of 3D boundary curves. The eigenvalues, trace values and determinants of the coefficient matrix are invariant to size, rotation and translation if the number of the sampled boundary data are fixed and are equally spaced. Coupling the orthogonal estimation algorithm with the extracted features of the eigenvalues, trace values and determinant provides a promising way of analysing and classifying 3D boundary curves.

References

ALOIMONOUS, J., WEISS, I., and BANDYOPADHYAY, A., 1987, Active vision, *Proc. IEEE Int. Conf. on Computer Vision*, 35-54.

BHANU, B., 1984, Representation and shape matching of 3D objects, *IEEE Trans. on Pattern Analysis and Machine Intelligence*, PAMI-6, 340-351.

DUBOIS, S.R., and GLANZ, F.H., 1986, An autoregressive model approach to two-dimensional shape classification, *IEEE Trans. on Pattern Analysis and Machine Intelligence*, PAMI-8, 55-66.

DUNDANI, S.A., BREEDINGS, K.J., and MCGHEE, R.B., 1977, Aircraft identification by moment invariants, *IEEE Trans. on Computers*, 26, 39-46.

JARVIS, R.A., 1983, A perspective on range finding techniques for computer vision, *IEEE Trans. on Pattern Analysis and Machine Intelligence*, PAMI-5, 122-139.

KREYSZIG, E., 1979, *Advanced Engineering Mathematics*, 4th ed., Wiley.

KORENBERG, M.J., BILLINGS, S.A. and LIU, Y.P., 1988, An orthogonal parameter estimation algorithm for nonlinear stochastic systems, *Int. J. Control*, 48, 193-210.

OSHIMA, M., and SHIRAI, Y., 1983, Object recognition using three dimensional information, *IEEE Trans. on Pattern Analysis and Machine Intelligence*, PAMI-5, 353-361.

SADJADI, F.A., and HALL, E.L., 1980, Three dimensional moment invariants, *IEEE Trans. on Pattern Analysis and Machine Intelligence*, PAMI-2, 127-136.

SEKITA, I., KURITA, T., and OTSU, N., 1992, Complex autoregressive model for shape recognition, *IEEE Trans. on Pattern Analysis and Machine Intelligence*, PAMI-14, 489-496.

TSANG, K.M., and BILLINGS, S.A., Two-dimensional pattern analysis and classification using a complex orthogonal estimation algorithm, *IEE Proc. Vision, Image and Signal Processing*, (in press).
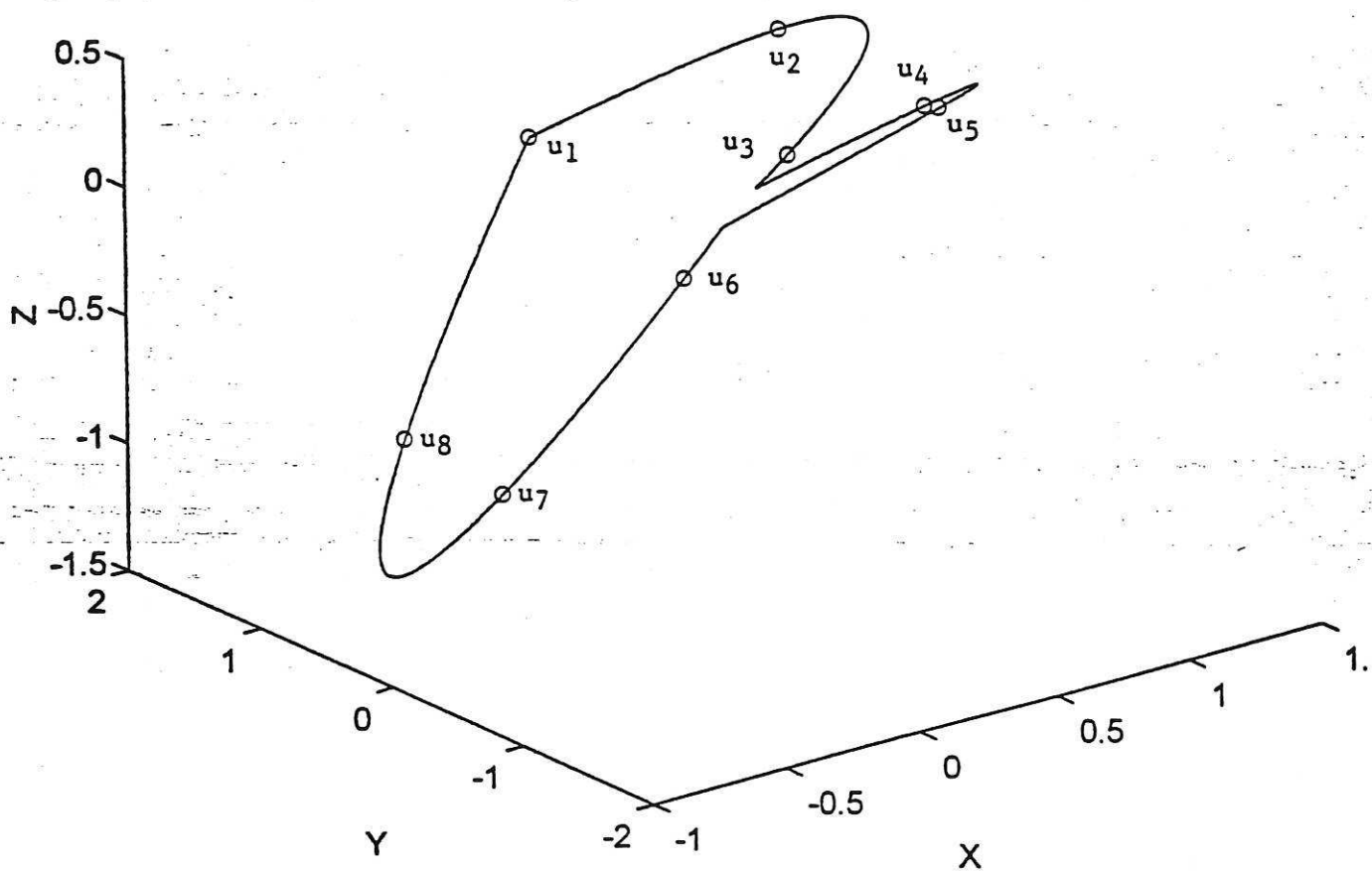
Figure 1. 3D boundary coordinates
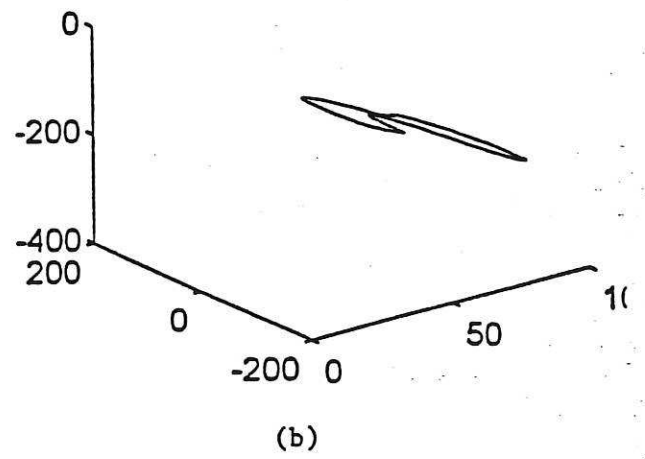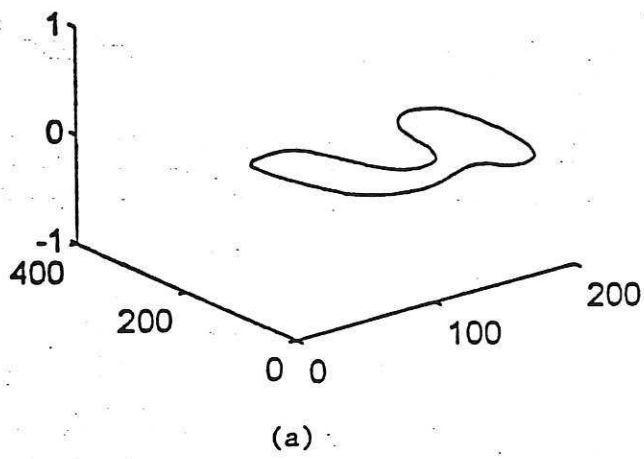
Figure 2. Plane shapes
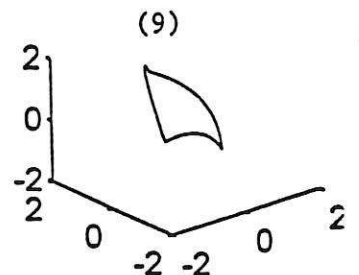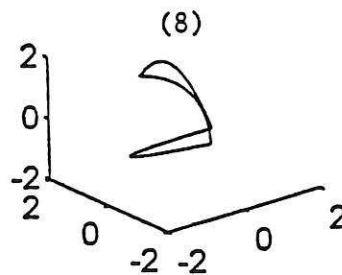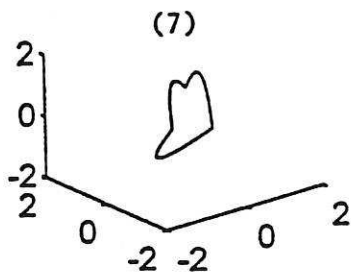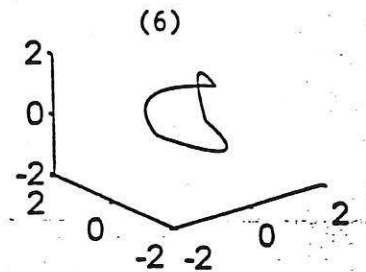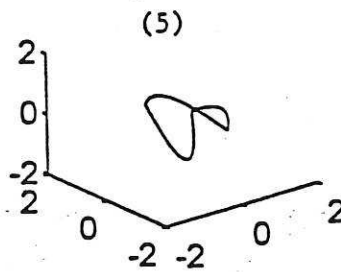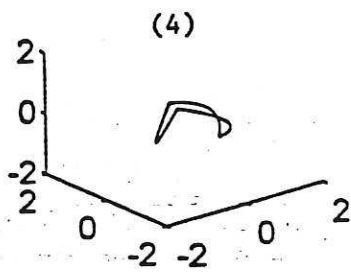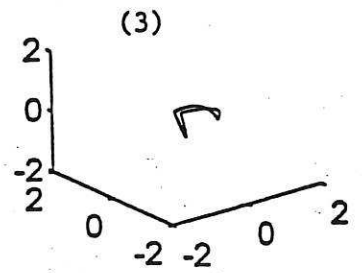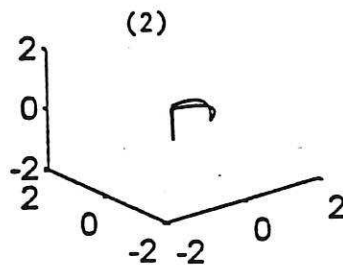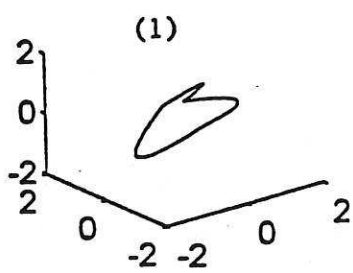
Figure 3. Shape set A
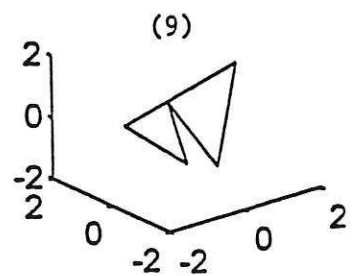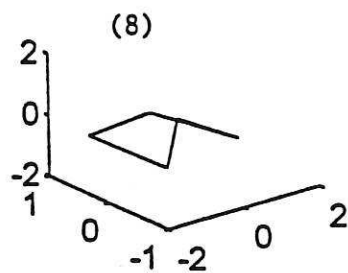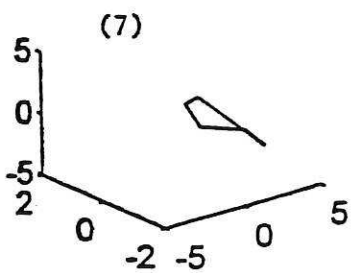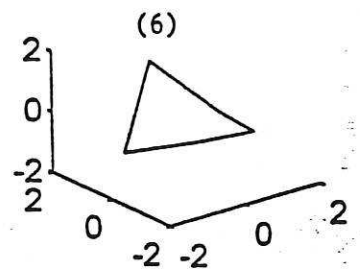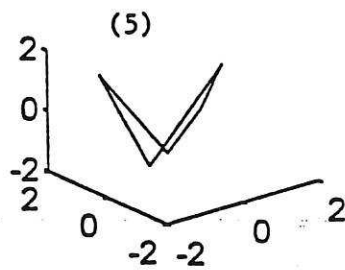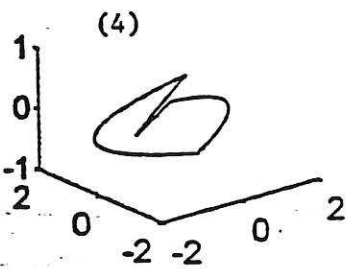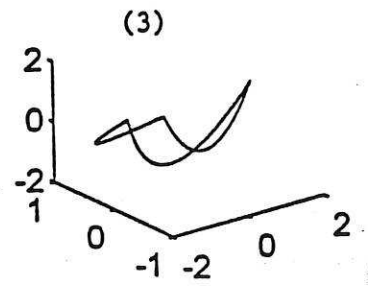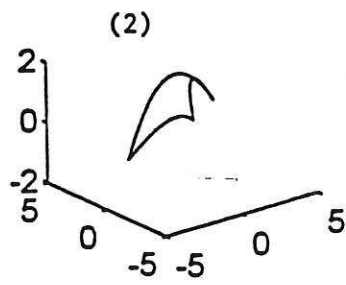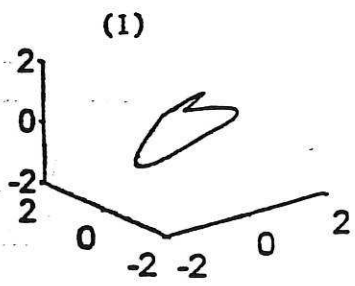
Figure 4. Shape set B
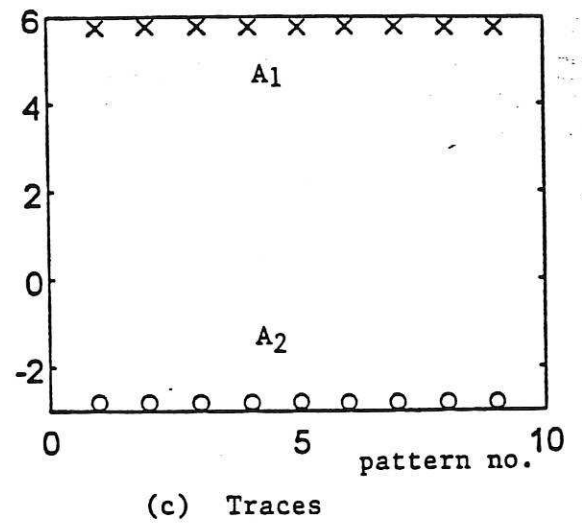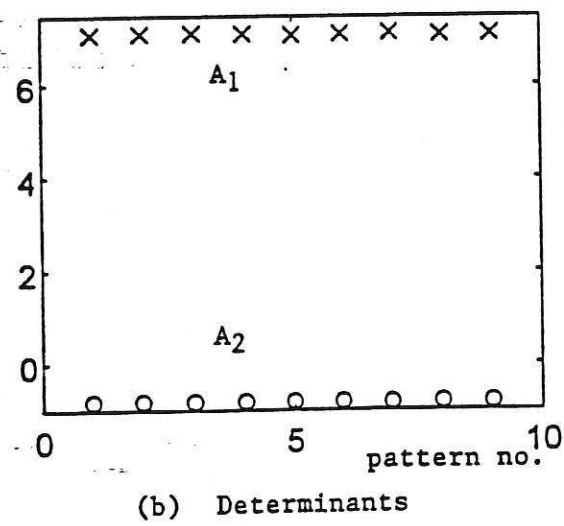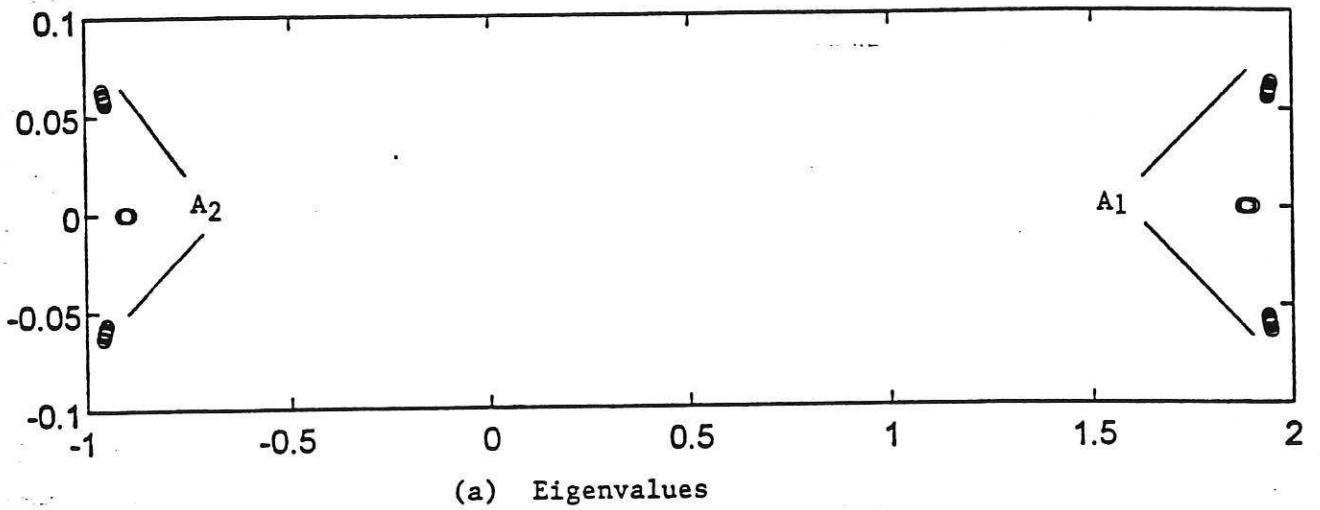
Figure 5. Eigenvalues, determinants and traces for shape set A
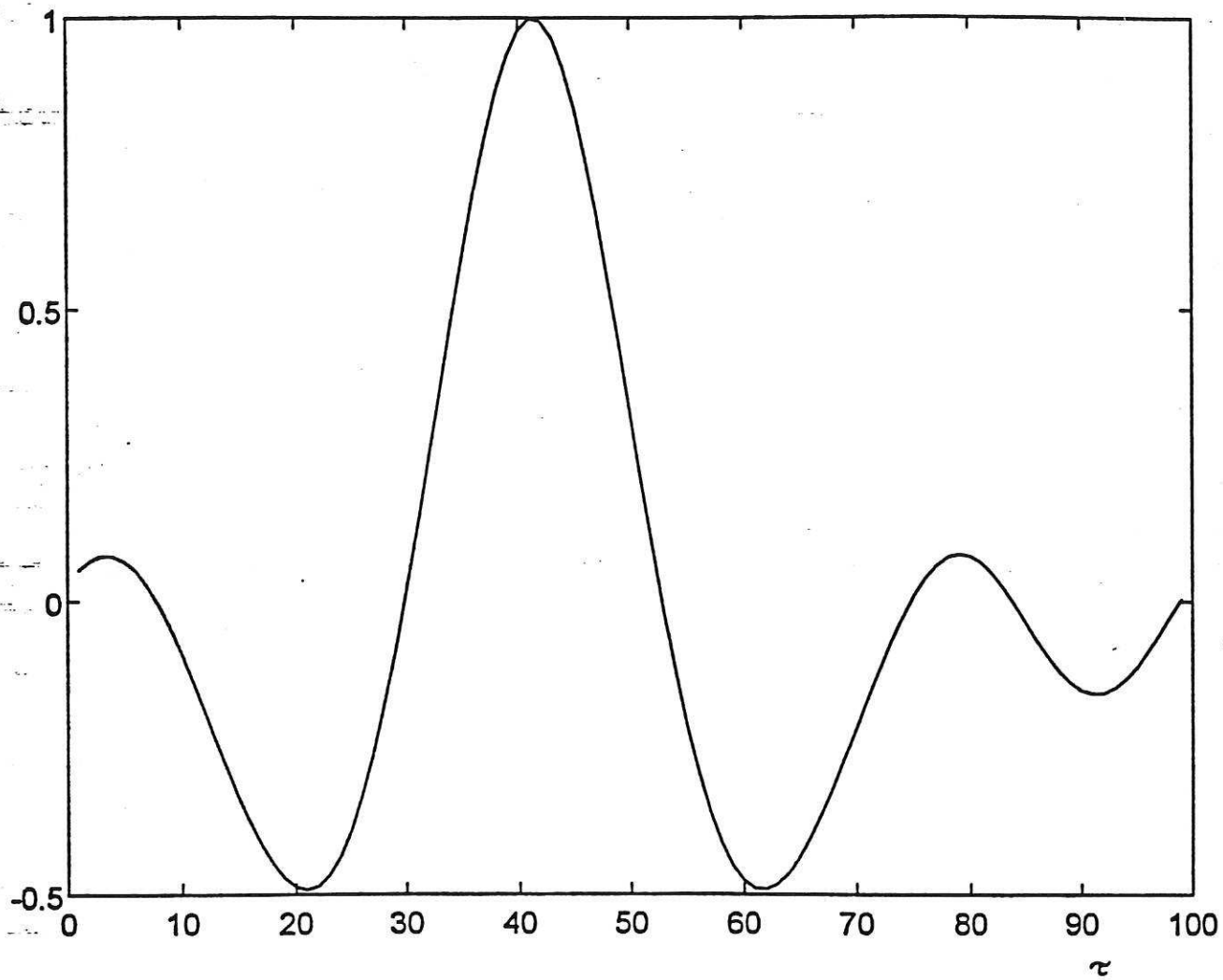
Figure 6.   Cross correlation function plot

Figure 7.   Transformed boundary points superimposed on
the actual data points

1 2 3 4 5 6 7 8 9 --- pattern no.

o + x ⊕ ⊠ ⊙ # * ⊖ --- symbols
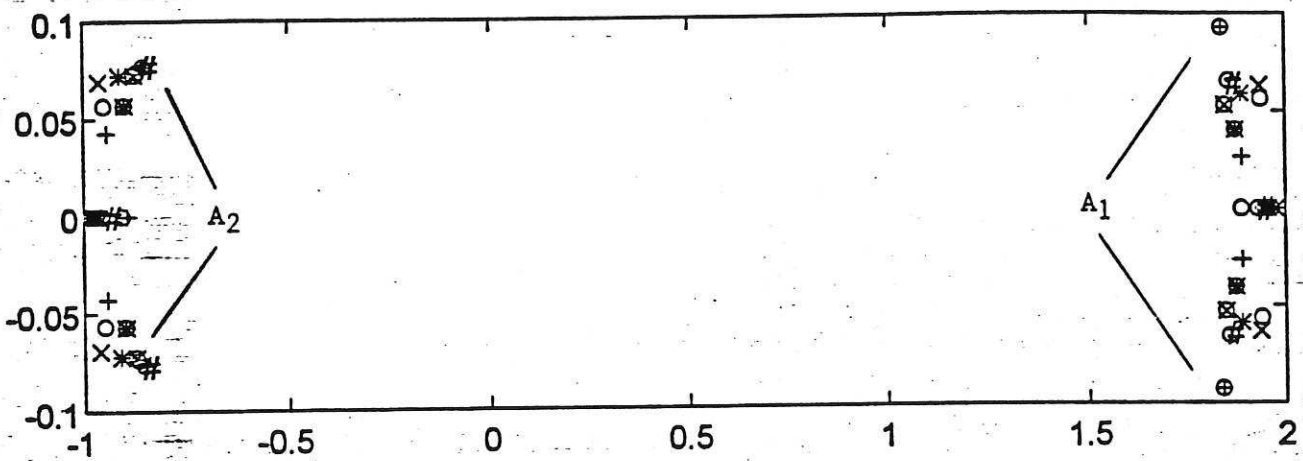
(a) Eigenvalues
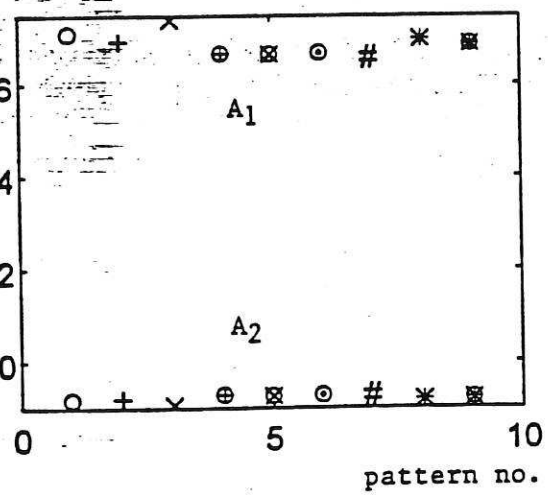
(b) Determinants
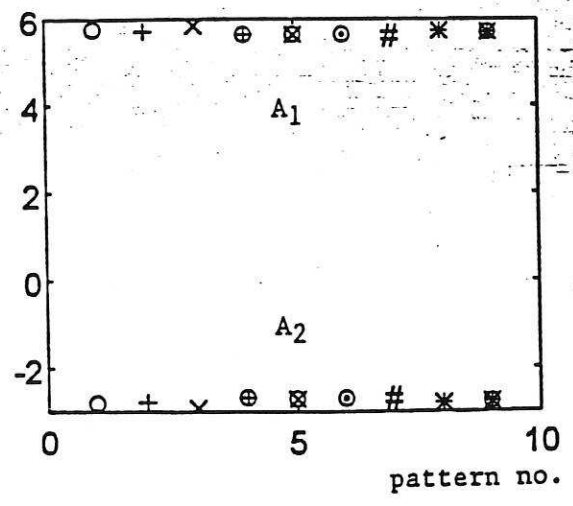
(c) Traces

Figure 8. Eigenvalues, determinants and traces for shape set B
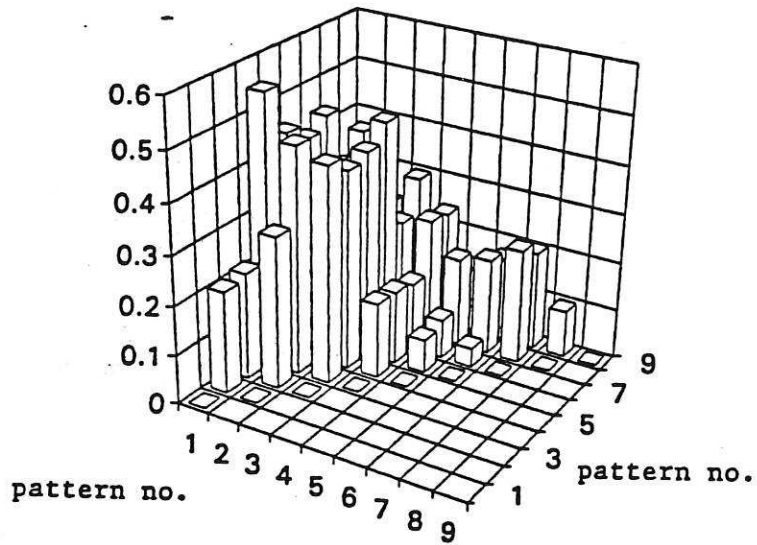
(a)   Eigenvalues
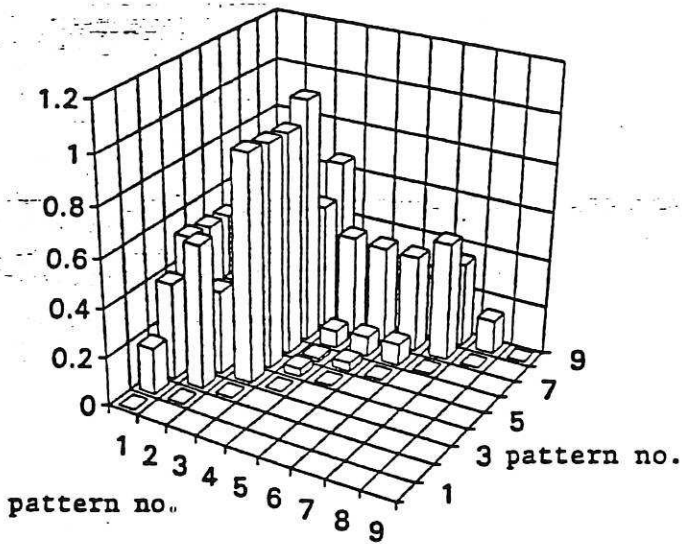
(b)   Determinants
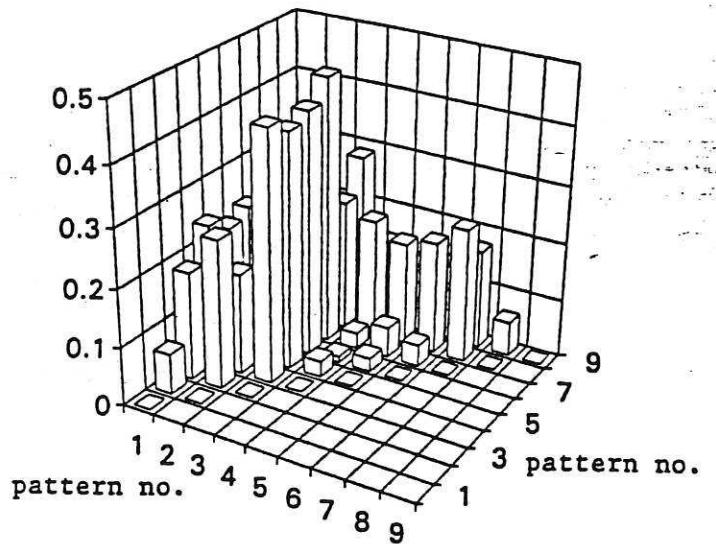
(c)   Traces

Figure 9.   Euclidean distances between the nine patterns of shape set B